Available online at www.sciencedirect.com
ScienceDirect
Trans. Nonferrous Met. Soc. China 22(2012) 255−261
Transactions of Nonferrous Metals Society of China
www.tnmsc.cn

Low temperature quasi-superplasticity of ZK60 alloy prepared by reciprocating extrusion

YANG Wen-peng[1], GUO Xue-feng[2], YANG Kai-jun[1]

1. School of Materials Science and Engineering, Xi'an University of Technology, Xi'an 710048, China;
2. School of Materials Science and Engineering, Henan Polytechnic University, Jiaozuo 454003, China

Received 11 April 2011; accepted 2 June 2011

Abstract: Fine-grained ZK60 alloy was prepared by 2-pass reciprocating extrusion, and the low temperature superplasticity was conducted in a temperature range from 443 to 523 K and an initial strain rate ranging from 3.3×10^{-4} to 3.3×10^{-2} s^{-1}. The results show that the alloy has an equiaxed grain structure with an average grain size of about 5.0 μm, and the sizes of broken secondary particles and precipitates are no more than 175 and 50 nm, respectively. The alloy exhibits quasi-superplasticity with a maximum elongation of 270% at 523 K and an initial strain rate of 3.3×10^{-4} s^{-1}. The strain rate sensitivity m is less than 0.2 at 443 and 473 K, and it is 0.42 at 523 K. The apparent activation energies at temperature below 473 K and at 523 K are less than 63.2 and 110.6 kJ/mol, respectively. At temperature below 473 K, mainly intragranular sliding contributes to superplastic flow. At 523 K, grain boundary sliding is the dominant deformation mechanism, and dislocation creep controlled by grain boundary diffusion is considered to be the main accommodation mechanism.

Key words: ZK60 Mg alloy; reciprocating extrusion; quasi-superplasticity; intragranular sliding; grain boundary sliding

1 Introduction

Mg alloys are becoming increasingly attractive for potential use in a wide range of engineering applications including aerospace and automobile industries because of their low density and high specific strength [1]. However, Mg alloys have hexagonal close-packed crystal structure in which the number of active slip systems is limited at room temperature. Therefore, Mg alloys have relatively low plasticity that severely restricts their applications. Development of fine- and ultrafine-grained Mg alloys prepared by means of severe plastic deformation, such as equal channel angular pressing (ECAP) [2−4] and reciprocating extrusion (RE) [5−7], is effective to improve the ductility of the materials both at room and elevated temperatures. RE appears to be a more versatile technique because it can effectively solve the problems of non-welding interfaces among rapidly solidified flakes [7] and powder in composites [8]; it can also facilitate to prepare fine-grained and homogeneous microstructure from as-cast ingot [9]. In general, Mg alloy with fine grains typically smaller than 10 μm facilitates the occurrence of superplastic deformation (elongation> 100%) at elevated temperature [10]. Recently, to achieve high strain rate superplasticity (HSRSP) ($\dot{\varepsilon} \geq 10^{-3}$ s^{-1}) at low temperature (from room temperature to 0.5 T_m, where T_m is the melting point of Mg), is especially attractive because Mg alloys have low formability at temperature close to room temperature and susceptibility to surface oxidation when deformed at elevated temperatures [11, 12]. ZK60 is a commercial Mg alloy, which has excellent superplasticity after being processed by ECAP [3, 4]. However, few reports have investigated the superplasticity of ZK60 alloy processed by RE. In the present study, the low temperature (≤523 K) superplastic behavior of fine-grained ZK60 alloy prepared by RE was studied, and the superplastic mechanism was discussed by theoretical calculations of strain rate sensitivity and activation energy.

Foundation item: Project (50271054) supported by National Natural Science Foundation of China; Project (20070700003) supported by Ph.D. Programs Foundation of Ministry of Education of China; Project (102102210031) supported by Science and Technologies Foundation of Henan, China; Project (2010A430008) supported by Natural Science Foundation of Henan Educational Committee, China
Corresponding author: YANG Wen-peng; Tel: +86-29-82314009; E-mail: wenpengy@gmail.com
DOI: 10.1016/S1003-6326(11)61168-0

2 Experimental

2.1 Materials

Commercial ZK60 alloy (Mg−5.47% Zn−0.25% Zr, mass fraction) was remelted in an electric resistance furnace at 993 K under Ar + SF_6 atmosphere. The ingots with dimensions of *d*22 mm×150 mm were prepared by pouring melt into graphite moulds. The as-cast ingots were machined into rods with dimensions of *d*20 mm×50 mm for extrusion. The principle of RE and detailed RE procedure can be found in Ref. [6]. Previous reports suggested that the material underwent 2-pass RE exhibited uniform fine-grained microstructure, and there was no remarkable microstructure refinement and mechanical property improvement with further increasing RE pass [6, 7]. Therefore, in the present study the ZK60 bullets were processed by 2-pass RE at 588 K under a ram speed of 1.0 mm/min. The total true strain provided for material by each RE pass is $\Delta\varepsilon=4\ln(d_0/d_m)$ [13], where d_0 is the inner diameter of the chamber and d_m is the diameter of the neck of the die. In this work, d_0=20 mm and d_m=6.4 mm were used. Hence, after 2-pass RE, the material had an accumulated true strain of about 9.2. The reciprocating extruded (REed) alloy was then extruded into cylindrical bar with a diameter of 6.4 mm at 573 K for convenient microstructural and mechanical property investigation.

2.2 Microstructural examination

Specimen cut from the extrusion bar for metallographic analysis was polished to mirror and etched in a reagent of 5% HNO_3 + 95% ethanol. The specimen was examined using a Niko Epiphot optical microscope (OM). The grain size of the alloy was measured by average linear intercept method. Specimens for transmission electron microscopy (TEM) investigation were twin-jet electron-polished to perforation in a solution of 11.2 g $Mg(ClO_4)_2$+5.3 g LiCl + 500 mL methanol+100 mL ethanol at 243 K, then ion-milled to remove the oxide film. The specimens were examined using a Philips CM30 TEM.

2.3 Superplastic behavior test

The dog-bone tensile specimens for superplastic deformation test were machined directly from cylindrical bars with tensile axis parallel to extruded direction. The specimens had a gauge length of 5 mm and cross-section area of 2 mm×3 mm. Uniaxial tensile tests were conducted in a temperature range between 443 and 523 K in air with constant cross-head speed. The initial strain rate range was from 3.3×10^{-4} to 3.3×10^{-2} s^{-1}. The cross-head speed of the 810 Material Test System and the temperature of the furnace attached to the MTS were controlled by a computer system with a Test Star IIs software. The heating time prior to the test was 30 min at 443 K, 40 min at 473 K and 60 min at 523 K, respectively. The fluctuations of the temperatures during test were ±2 K at 443 K and 473 K, ±5 K at 523 K, respectively. The fractures were examined on a Philips XL30 scanning electron microscope (SEM).

3 Results

Figure 1 shows the microstructure of the REed ZK60 alloy. The OM image (Fig. 1(a)) taken from cross section shows that the microstructure of REed alloy is reasonably homogeneous and consists of equiaxed fine grains with an average grain size of 5.0 μm. It is suggested that the as-cast alloy was heavily deformed and the recrystallization occurred during the RE process. Bright-field TEM micrograph (Fig. 1(b)) reveals that the small broken secondary phase particles distributed within grains and at grain boundaries are smaller than 175 nm, and the sizes of precipitates homogeneously dispersed within grains are smaller than 50 nm. It is noted that the mainly compound particles in ZK60 alloy are Mg_7Zn_3, $MgZn_2$ and Mg_4Zn_7 [14, 15].

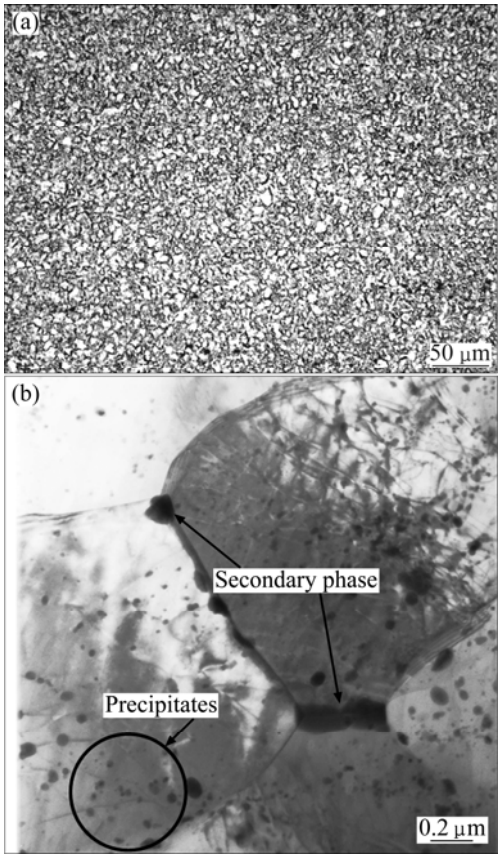

Fig. 1 Microstructure of REed ZK60 alloy: (a) OM image showing uniform fine grain microstructure; (b) Bright-field TEM image showing broken secondary phase particles and precipitates

Figure 2 shows the representative plots of the true stress—true strain curves for the REed ZK60 alloy. Under various test conditions, the flow stress increases firstly to the peak stress (σ_p) and then decreases to failure. The increase of strength during test can be correlated with low density of mobile dislocations, while the strength increases to σ_p, and the flow stress decreases due to dislocations multiplication and cross-slip [16]. At 443 and 473 K, the flow stress increases to a maximum and then decreases rapidly to failure in a wide strain hardening range. When deformed at 523 K and low initial strain rate of 3.3×10^{-4} s^{-1}, the flow stress firstly increases to σ_p and then slight decreases to a steady state value with increasing strain. In addition, compared with smooth stress — strain curves obtained in many superplastic materials [17, 18], an additional oscillation of flow stress observed under all deformation conditions should be caused by the dynamic interaction of solute atoms with mobile dislocations [19].

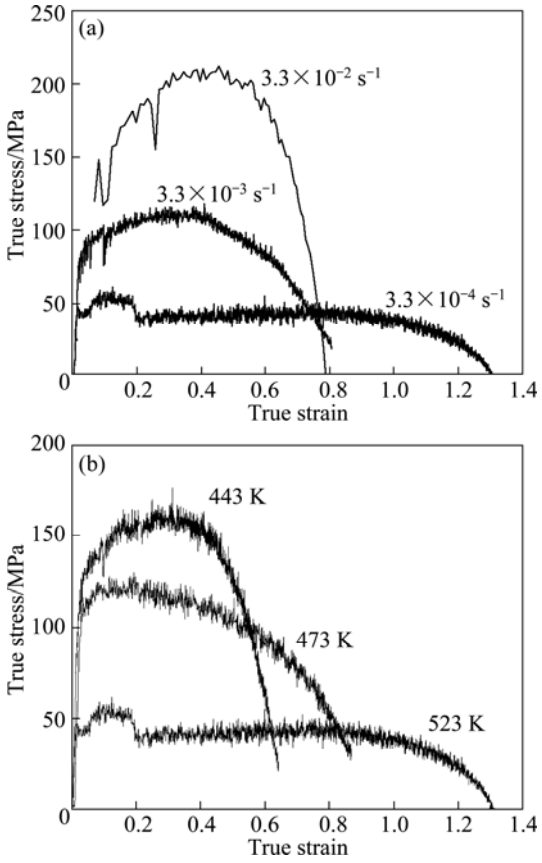

Fig. 2 Typical true stress—true strain curves of REed ZK60 alloy: (a) At 523 K and various strain rates; (b) At initial strain rate of 3.3×10^{-4} s^{-1} and various temperatures

The variation of elongation-to-failure as a function of temperature is summarized in Fig. 3. It is apparent that at low initial strain rate of 3.3×10^{-4} s^{-1}, the increase of elongation is considerably large with increasing temperature. A maximum elongation of 270% is achieved at 523 K. However, at relatively high strain rates of 3.3×10^{-3} and 3.3×10^{-2} s^{-1}, the effect of temperature on elongation is weak. It is noted that the elongations for the specimens tested at temperature of 473 K and initial strain rates of 3.3×10^{-3} and 3.3×10^{-2} s^{-1} are larger than 100%, indicating that the low temperature super plasticity and HSRSP are achieved simultaneously in the REed ZK60 alloy.

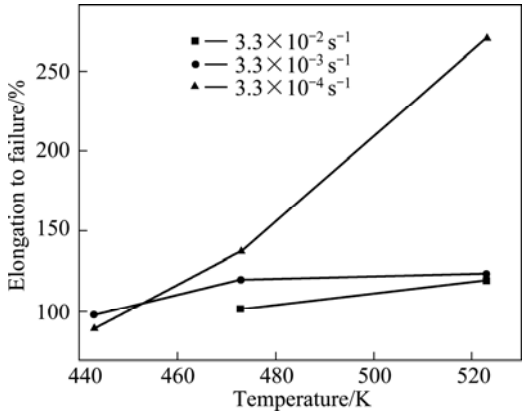

Fig. 3 Variations of elongation-to-failure as function of temperature

Figure 4 illustrates the original dog-bone specimen and a group of fractured specimens pulled to failure at 523 K at different initial strain rates. All the specimens are failed by plastic necking before fracture.

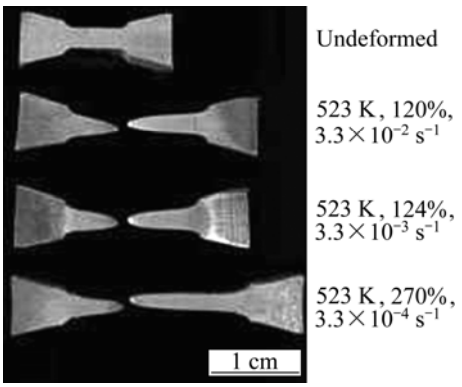

Fig. 4 Original and tensile fractured specimens of REed ZK60 alloy

The fracture morphologies of the specimens tested at initial strain rate of 3.3×10^{-4} s^{-1} and various temperatures are shown in Fig. 5. For the specimens tested at 443 and 523 K, the fractures are composed of equiaxed deep holes and a few dimples. It can be concluded that most grains were pulled out completely from the deep holes and a few grains were fractured intergranularly. At 523 K, the fracture is composed of deep holes and the ductile dimple cannot be observed. The average sizes of deep holes for specimens tested at

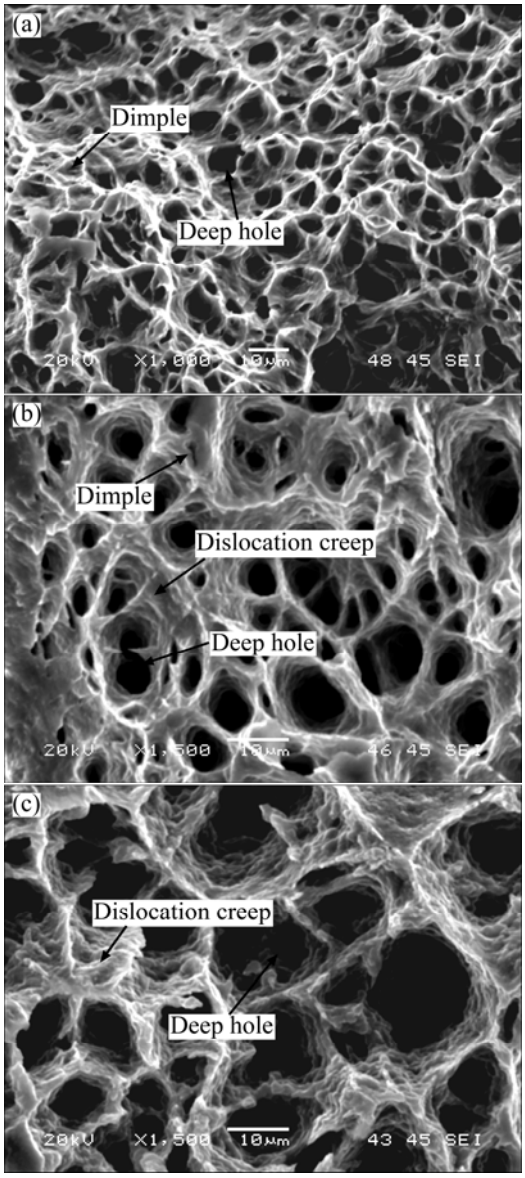

Fig. 5 SEM images obtained from fractures of specimens tested at initial strain rate of 3.3×10^{-4} s^{-1} and temperatures of 443 K (a), 473 K (b) and 523 K (b)

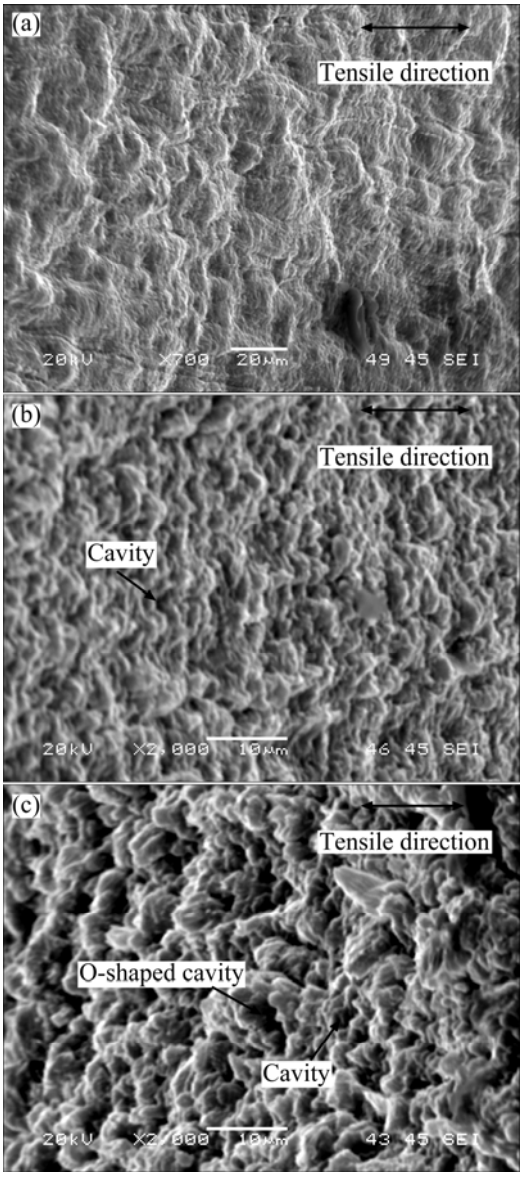

Fig. 6 SEM images obtained from surfaces near fractures of specimens tested at initial strain rate of 3.3×10^{-4} s^{-1} and temperatures of 443 K (a), 473 K (b) and 523 K (c)

443, 473 and 523 K are 5.0, 5.5 and 10.0 μm, respectively. The enlarged holes with increasing temperatures are mostly attributed to the grain growth at elevated temperatures. In addition, for the specimens tested at 473 and 523 K, some tearing edges around the deep holes are observed.

Figure 6 shows the surface flowabilities of tested specimens along tensile direction. It is clear that the flowability is gradually obvious as test temperature increases. There is no evident flowability for the specimen tested at 443 K. Slight flowability and a few cavities can be found when tested at 473 K. At 523 K, evident flowability throughout the gauge region is observed and there are many O-shaped cavities distributed on the surface.

4 Discussion

The largest elongation attained in the present study is 270%, which is lower than that of the fine-grained ZK60 alloy previously reported [10, 11]. Except for the relatively low test temperature, one of the most important reasons is the effect of grain size, because the reduction in grain size cannot only increase the optimum strain rate for the maximum elongation but also increase the value of elongation. WATANABE et al [11] suggested that the required grain size for true HSRSP at low temperatures is 0.4 μm. It is also indicated that the decrease in grain size could decrease the temperature for optimum superplastic flow. Hence, the grain size of 5.0 μm is relatively large to attain the true superplasticity at low temperatures.

The equation to describe diffusion assisted with high temperature mechanical behavior is generally expressed as [20]:

$$\dot{\varepsilon} = \frac{AD_0Eb}{kT}\left(\frac{\sigma}{E}\right)^n\left(\frac{b}{d}\right)^p \exp\left(\frac{-Q}{RT}\right) \quad (1)$$

where $\dot{\varepsilon}$ is the strain rate; σ is the flow stress; A is a constant dependent on material parameters; d is the average grain size; Q is the appropriate activation energy for rate-limiting process; n is the stress exponent (reciprocal to the strain rate sensitivity m, i.e., $m = 1/n$); p is the inverse grain size exponent; D_0 is the pre-exponential factor of diffusivity; T is the temperature; E is the elastic modulus; b is the Burgers vector; k is the Boltzmann's constant; R is the universal gas constant.

To characterize the effects of strain rate on the behavior of plastic flow, the variation in flow stress as a function of initial strain rate is plotted in Fig. 7, where the flow stress for each strain rate is determined at a small strain of $\varepsilon = 0.2$. Under such a small strain, grain growth during initial superplastic flow stage is negligible. It is demonstrated that for many superplastic materials, the flow stress increases with increasing strain rate in a typical sigmoidal curve [12, 17]. However, the sigmoidal curves in the present study are not complete because the test conditions are restricted at low temperatures and relatively high strain rates. The strain rate sensitivity exponent m, defined as the slop of the double logarithmic plot of flow stress versus strain rate, is 0.42 at low initial strain rates at 523 K. It is well accepted that grain boundary sliding (GBS) is the dominant deformation mechanism for Mg alloy superplastic flow with a high m value of about 0.5 [12, 21]. This is because if necking begins to occur in a material with a high m, the necked region strains at a higher rate. The higher strain rate in turn strengthens the necked region, stops the necking and permits uniform deformation to continue. However, the specimen tested at 523 K is failed by plastic necking. Hence, the adequate elongation is attributed to the advent of quasi-superplastic flow. At low temperatures (443 and 473 K), the m-values are smaller than 0.2. Such a small value indicates the existence of a high threshold stress, that is, the dislocations dominate the deformation [22].

In order to understand the deformation mechanisms during superplastic process, the apparent superplastic deformation activation energy Q_a is calculated under constant strain rate as follows [5]:

$$Q_a = Rn\frac{\partial(\ln\sigma)}{\partial(1/T)} \quad (2)$$

where R is the gas constant; T is the temperature; $\partial(\ln\sigma)/\partial(1/T)$ is estimated from the slop of the curve in Fig. 8. It is demonstrated that the slopes of curves increase with increasing temperatures and decreasing strain rates. At 443 and 473 K, the maximum of Q_a is (63.2±4.0) kJ/mol, which is lower than that for grain boundary diffusion in pure Mg of 92 kJ/mol [23]. This is reasonable to suggest that intragranular sliding (IGS) contributes to the superplastic flow, which is confirmed from the SEM observations of fracture surfaces (Fig. 6). At 523 K, the activation energy is determined to be (110.6±30.8) kJ/mol, which is between that for lattice self-diffusion in pure Mg of 135 kJ/mol [23] and that for grain boundary diffusion. The deformation mechanism is considered to be GBS accommodated by slip controlled by grain boundary diffusion. It is consistent with the SEM observations of the fracture, as shown in Figs. 5(c) and 6(c). In addition, the tearing edges around the deep holes in Figs. 5(b) and (c) are originated from atom diffusion in grains or around grain boundaries and develop in the form of dislocation creep. Therefore, dislocation creep may continuously play a critical role in superplastic deformation.

The threshold stress has been suggested to exist and vary with temperature. Equation (3) is used to calculate the

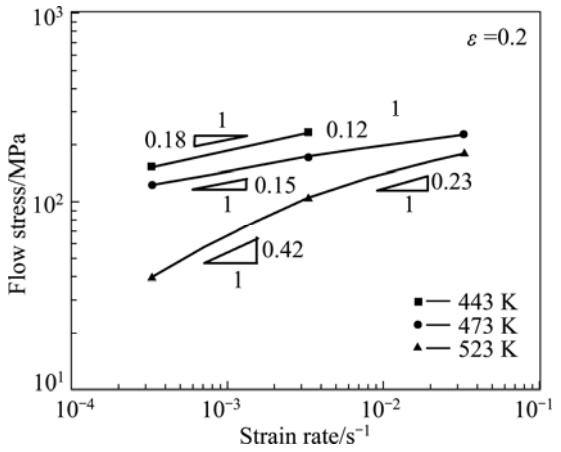

Fig. 7 Flow stress as function of strain rate for REed ZK60 alloy

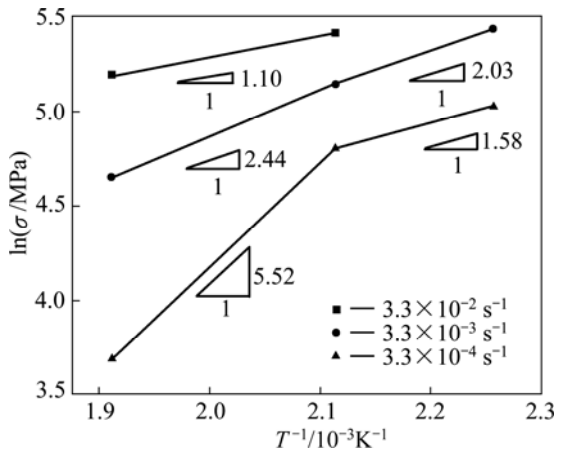

Fig. 8 Activation energy curves of lnσ vs $1/T$ in superplasticity deformation of REed ZK60 alloy

threshold stress as [22]:

$$\dot{\varepsilon}=\frac{ADGb}{kT}\left(\frac{b}{d}\right)^{p}\left(\frac{\sigma-\sigma_0}{G}\right)^{n} \tag{3}$$

where D is the diffusion coefficient; G is the shear modulus; σ_0 is the threshold stress. The n is determined as 2, 3 and 5 in the plot of $\dot{\varepsilon}^{1/n}$ against σ, and then the best values of n that yields the best linear fitting are chosen. The best linear fitting occurs at n = 2 (the linear fitting for n = 3 and 5 are not shown), and the threshold stress at $\dot{\varepsilon}$=0 are calculated to be 120.3, 119.6 and 35.6 MPa at 443, 473 and 523 K, respectively, as shown in Fig. 9.

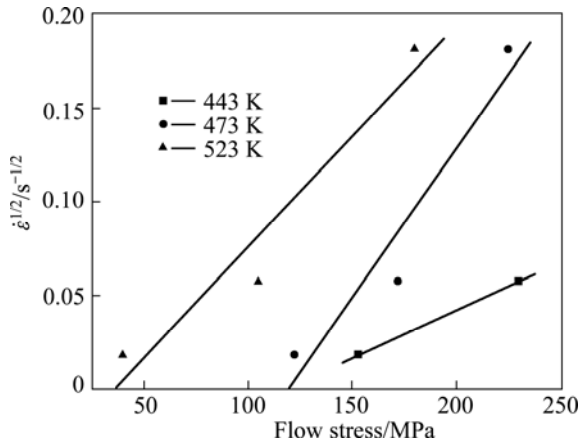

Fig. 9 $\dot{\varepsilon}^{1/2}$ at various test temperatures as function of flow stress

The high threshold stress of about 120 MPa at 443 and 473 K could result from the twinning and dislocation slip during superplastic process. The elongations below 473 K are considered to be the contribution of non-basal dislocation slip. KOIKE et al [24] investigated the deformed microstructure of AZ31B Mg alloy with an average grain size of 6.5 μm at room temperature and found that non-basal segment of dislocations is about 40% in the total dislocations. This was also confirmed by GALIYEV et al [25]. In their study, twinning, basal slip and non-basal dislocation slip were found to be operated at temperature below 473 K. In addition, the formation mechanism of the small cavities observed in Fig. 6(b) belongs to conventional mode, in which the cavities originate from the secondary phase particles or inclusions and develop with the detachment between them.

The low threshold stress at 523 K is attributed to the GBS. In general, during GBS process, stress concentrations are caused at ledges along grain boundaries and at triple junctions of grain boundaries [21]. The threshold stress could result from the transformation of gliding grain boundary dislocations according to the model proposed by GUTKIN et al [26]. In order to relax the stress concentrations and accommodate GBS, dislocations are generated at ledges along grain boundaries and at triple junctions of grain boundaries [22]. With the deformation increasing, grain boundaries become more and more difficult to slide and the contribution of GBS is little to deformation. Therefore, an accommodating mechanism is needed to slide continually. In turn, the dislocation creep controlled by grain boundary diffusion acts as the accommodating mechanism and has a contribution to superplastic deformation in the final stage. Therefore, evident flowability through the gauge region could be observed, as shown in Fig. 6(c). Moreover, there are many O-shaped cavities and cavity coalescences distributed on the specimen surface. The minute cavities form at grain boundaries and triple junctions of grain boundaries. The minute cavities experience the growth and moving under the control of grain boundaries diffusion. Finally, the interlinkage of intergranular cavities results in the failure of the specimen.

5 Conclusions

1) ZK60 alloy processed by 2-pass reciprocating extrusion is completely recrystallized. The microstructure consists of fine grains, broken secondary phase particles and precipitates.

2) The alloy exhibits the quasi-superplastic behavior, the maximum elongation of 270% is achieved at 523 K with an initial strain rate of 3.3×10^{-4} s^{-1}.

3) The value of strain rate sensitivity m is less than 0.2 at tensile temperatures below 523 K, and it is up to 0.42 at 523 K. The apparent activation energies Q_a at temperature lower than 273 K and at 523 K are less than 63.2 and 110.6 kJ/mol, respectively. The threshold stresses at 443, 473 and 523 K are calculated to be 120.3, 119.6 and 35.6 MPa, respectively.

4) At temperature lower than 473 K, the superplastic flow mechanism is intragranular sliding; at 523 K, the dominant deformation mechanism is grain boundary sliding, and the dislocation creep controlled by grain boundary diffusion is the main accommodation mechanism.

References

[1] FROES F H. Advanced metals for aerospace and automotive use [J]. Materials Science and Engineering A, 1994, 184(2): 119−133.

[2] MATSUBARA K, MIYAHARA Y, HORITA Z, LANGDON T G. Developing superplasticity in a magnesium alloy through a combination of extrusion and ECAP [J]. Acta Materialia, 2003, 51(11): 3073−3084.

[3] WATANABE H, MUKAI T, ISHIKAWA K, HIGASHI K. Low temperature superplasticity of a fine-grained ZK60 magnesium alloy processed by equal-channel-angular extrusion [J]. Scripta Materialia, 2002, 46(12): 851−856.

[4] FIGUEIREDO R B, LANGDON T G. The development of superplastic ductilities and microstructural homogeneity in a magnesium ZK60 alloy processed by ECAP [J]. Materials Science and Engineering A, 2006, 430(1−2): 151−156.
[5] LEE S W, CHEN Y L, WANG H Y, YANG C F, YEH J W. On mechanical properties and superplasticity of Mg−15Al−1Zn alloys processed by reciprocating extrusion [J]. Materials Science and Engineering A, 2007, 464(1−2): 76−84.
[6] GUO X F, SHECHTMAN D. Reciprocating extrusion of rapidly solidified Mg−6Zn−1Y−0.6Ce−0.6Zr alloy [J]. Journal of Materials Processing Technology, 2007, 187−188: 640−644.
[7] GUO X F, REMENNIK S, XU C, SHECHTMAN D. Development of Mg−6.0%Zn−1.0%Y−0.6%Ce−0.6%Zr magnesium alloy and its microstructural evolution during processing [J]. Materials Science and Engineering A, 2008, 473(1−2): 266−273.
[8] CHU H S, LIU K S, YEH J W. An in situ composite of Al (graphite, Al_4C_3) produced by reciprocating extrusion [J]. Materials Science and Engineering A, 2000, 277(1−2): 25−32.
[9] CHEN Y J, WANG Q D, ROVEN H J, LIU M P, KARLSEN M, YU Y D, HJELEN J. Network-shaped fine-grained microstructure and high ductility of magnesium alloy fabricated by cyclic extrusion compression [J]. Scripta Materialia, 2008, 58(4): 311−314.
[10] MABUCHI M, IWASAKI H, YANASE K, HIGASHI K. Low temperature superplasticity in an AZ91 magnesium alloy processed by ECAE [J]. Scripta Materialia, 1997, 36(6): 681−686.
[11] WATANABE H, MUKAI T, ISHIKAWA K, MABUCHI M, HIGASHI K. Realization of high-strain-rate superplasticity at low temperatures in a Mg−Zn−Zr alloy [J]. Materials Science and Engineering A, 2001, 307(1−2): 119−128.
[12] WANTANABE H, MUKAI T, MABUCHI M, HIGASHI K. High-strain-rate superplasticity at low temperature in a ZK61 magnesium alloy produced by powder metallurgy [J]. Scripta Materialia, 1999, 41(2): 209−213.
[13] RICHERT M, STÜWE H P, ZEHETBAUER M J, RICHERT J, PIPPAN R, MOTZ C, SCHAFLER E. Work hardening and microstructure of AlMg5 after severe plastic deformation by cyclic extrusion and compression [J]. Materials Science and Engineering A, 2003, 355(1−2): 180−185.
[14] GAO X, NIE J F. Characterization of strengthening precipitate phases in a Mg−Zn alloy [J]. Scripta Materialia, 2007, 56(8): 645−648.
[15] GAO X, NIE J F. Structure and thermal stability of primary intermetallic particles in an Mg−Zn casting alloy [J]. Scripta Materialia, 2007, 57(7): 655−658.
[16] CHEZAN A R, DeHOSSON J T M. Superplastic behavior of coarse-grained aluminum alloys [J]. Materials Science and Engineering A, 2005, 410−411: 120−123.
[17] WEI Y H, WANG Q D, ZHU Y P, ZHOU H T, DING W J, CHINO Y, MABUCHI M. Superplasticity and grain boundary sliding in rolled AZ91 magnesium alloy at high strain rates [J]. Materials Science and Engineering A, 2003, 360(1−2): 107−115.
[18] LEE J Y, LIM H K, KIM D H, KIM W T, KIM D H. Effect of volume fraction of quasicrystal on the mechanical properties of quasicrystal-reinforced Mg−Zn−Y alloys [J]. Materials Science and Engineering A, 2007, 449−451: 987−990.
[19] CORBY C, CÁCERES C, LUKÁČ P. Serrated flow in magnesium alloy AZ91 [J]. Materials Science and Engineering A, 2004, 387−389(1−2): 22−24.
[20] CHARIT I, MISHRA R S. Low temperature superplasticity in a friction-stir-processed ultrafine grained Al−Zn−Mg−Sc alloy [J]. Acta Materialia, 2005, 53(15): 4211−4223.
[21] WANG Y N, HUANG J C. Comparison of grain boundary sliding in fine grained Mg and Al alloys during superplastic deformation [J]. Scripta Materialia, 2003, 48(8): 1117−1122.
[22] MABUCHI M, AMEYAMA K, IWASAKI H, HIGASHI K. Low temperature superplasticity of AZ91 magnesium alloy with non-equilibrium grain boundaries [J]. Acta Materialia, 1999, 47(7): 2047−2057.
[23] CHUVIL'DEEV V N, NIEH T G, GRYAZNOV M Y, KOPYLOV V I, SYSOEV A N. Superplasticity and internal friction in microcrystalline AZ91 and ZK60 magnesium alloys processed by equal-channel angular pressing [J]. Journal of Alloys and Compounds, 2004, 378(1−2): 253−257.
[24] KOIKE J, KOBAYASHI T, MUKAI T, WATANABE H, SUZUKI M, MARUYAMA K, HIGASHI K. The activity of non-basal slip systems and dynamic recovery at room temperature in fine-grained AZ31B magnesium alloys [J]. Acta Materialia, 2003, 51(7): 2055−2065.
[25] GALIYEV A, KAIBYSHEV R, GOTTSTEIN G. Correlation of plastic deformation and dynamic recrystallization in magnesium alloy ZK60 [J]. Acta Materialia, 2001, 49(7): 1199−1207.
[26] GUTKIN M Y, OVID'KO I A, SKIBA N V. Strengthening and softening mechanisms in nanocrystalline materials under superplastic deformation [J]. Acta Materialia, 2004, 52(6): 1711−1720.

往复挤压 ZK60 合金的低温准超塑性

杨文朋[1]，郭学锋[2]，杨凯军[1]

1. 西安理工大学 材料科学与工程学院，西安 710048；
2. 河南理工大学 材料科学与工程学院，焦作 454003

摘 要：通过 2 道次往复挤压制备细晶 ZK60 合金，在 443~523 K 和初始应变速率为 3.3×10^{-4}~3.3×10^{-2} s^{-1} 的范围内测试合金的低温超塑性。结果表明：往复挤压 ZK60 合金的平均晶粒尺寸约为 5.0 μm，分布于基体内的破碎二次相颗粒和沉淀颗粒尺寸分别为不大于 175 nm 和 50 nm。该合金具有低温准超塑性，在 523 K 和 3.3×10^{-4} s^{-1} 应变速率下伸长率最大，为 270%；在 443 和 473 K 时，应变速率敏感系数 m 小于 0.2；在 523 K 时 m 为 0.42。当温度不高于 473 K 和 523 K 时，超塑性变形激活能分别不高于 63.2 kJ/mol 和 110.6 kJ/mol。当低于 473 K 时，主要的超塑性流变机制为晶内滑移；在 523 K 时，主要的超塑性变形机制为晶界滑移，由晶界扩散控制的位错蠕变为主要的兼容机制。

关键词：ZK60 镁合金；往复挤压；准超塑性；晶内滑移；晶界滑移

(Edited by FANG Jing-hua)